Environmental Pollution 333 (2023) 121996

Contents lists available at ScienceDirect

Environmental Pollution

journal homepage: www.elsevier.com/locate/envpol

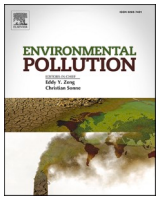

Effect of paper filter windows on indoor exposure to particles of outdoor origin☆

Suwhan Yee [a], Jason Spitzack [b], Jacob Swanson [b], Heejung Jung [c], Donghyun Rim [a,*]

[a] Department of Architectural Engineering, Pennsylvania State University, University Park, PA, USA
[b] Department of Integrated Engineering, Minnesota State University, Mankato, MN, USA
[c] Department of Mechanical Engineering, University of California, Riverside, CA, USA

ARTICLE INFO

Keywords:
Indoor air quality
Contaminants
Particle control
Building ventilation
Wildfire

ABSTRACT

Buildings are often located near ambient air pollution sources such as wildfire or heavy traffic areas. While windows in buildings are intermittently open for free cooling or natural ventilation, increased leakage area can lead to elevated human exposure to air pollutants of outdoor origin. The objective of this study is to investigate the effectiveness of paper filter windows in reducing exposure to outdoor air pollution and improving indoor air quality. The physical properties of paper windows as filtration media were experimentally determined, based on which multi-zone indoor air quality and ventilation analysis (CONTAM) simulations were performed for a full-scale building. The results show that the outdoor-indoor air exchange rate of a building can increase about 100% when conventional windows are replaced with paper filter windows. Even with the increased air exchange rate, the infiltration of outdoor particles into the building was reduced about 57–77% for the particle size range of 7–300 nm. These findings imply that paper windows have potential benefits for controlling both outdoor originated pollutants and indoor-generated pollutants with minimal energy inputs, especially in cities and communities impacted by urban air pollution and wildfires.

1. Introduction

Indoor air quality is closely related to human health and comfort (McGuinn et al., 2017; Stabile et al., 2017; Turanjanin et al., 2014). People spend most of their time indoors while being exposed to indoor air pollutants (Klepeis et al., 2001; Schweizer et al., 2007). A number of previous studies determined human exposure to pollutants of outdoor origin as well as indoor chemicals (Gall et al., 2015; Licina et al., 2017; Marshall et al., 2006; Mullen et al., 2011a; Mullen et al., 2011b; Rim et al., 2017). According to the United States Environmental Protection Agency (USEPA), more than 45 million people in the U.S. live within 90 m of a central transportation facility or infrastructure (Quiros et al., 2013). The exposure to outdoor originated fine particles could increase up to 200% near transportation infrastructures and up to 40 times higher levels during wildfire events (Chen et al., 2021; Wang and Gao, 2011). Human inhalation exposure to airborne particles is associated with an increased risk of lung cancer and cardiovascular diseases that increase mortality, especially for those exposed to an extreme level of particles more than 50 days a year (Brook et al., 2010; Ristovski et al., 2012).

Windows in residential buildings are intermittently open for ventilation and space conditioning. As a result, pollutants of outdoor origin can penetrate indoors and affect human exposure to particles. Dutton et al. (2013) studied that health cost of natural ventilation are closely associated with adverse health effects of ozone and particulate matter smaller than 2.5 μm ($PM_{2.5}$). According to United States Census Bureau's technical document B25035, the median built year of American buildings is 1978. As more than half of the buildings were built over 40 years ago, many old buildings are not airtight, even with windows closed (Yamamoto et al., 2010). Furthermore, Ruan and Rim (2019) reported that the indoor concentration of $PM_{2.5}$ is closely related to ventilation flow rates and filter efficiency installed in the ventilation system.

Xiang et al. (2019) estimated, based on data collection from about 1500 monitoring sites in 339 Chinese cities, that indoor exposure to $PM_{2.5}$ of outdoor origin accounted for 66%–87% of total exposure to $PM_{2.5}$. They also reported that decreasing indoor concentrations of outdoor-originated $PM_{2.5}$ is essential, and ventilation or filtration systems should be further improved to reduce the annual average indoor $PM_{2.5}$ concentration. Various types of ventilation and filtration systems

☆ This paper has been recommended for acceptance by Sumin Kim.

* Corresponding author.
E-mail address: drim@psu.edu (D. Rim).

https://doi.org/10.1016/j.envpol.2023.121996
Received 5 February 2023; Received in revised form 28 May 2023; Accepted 8 June 2023
Available online 17 June 2023

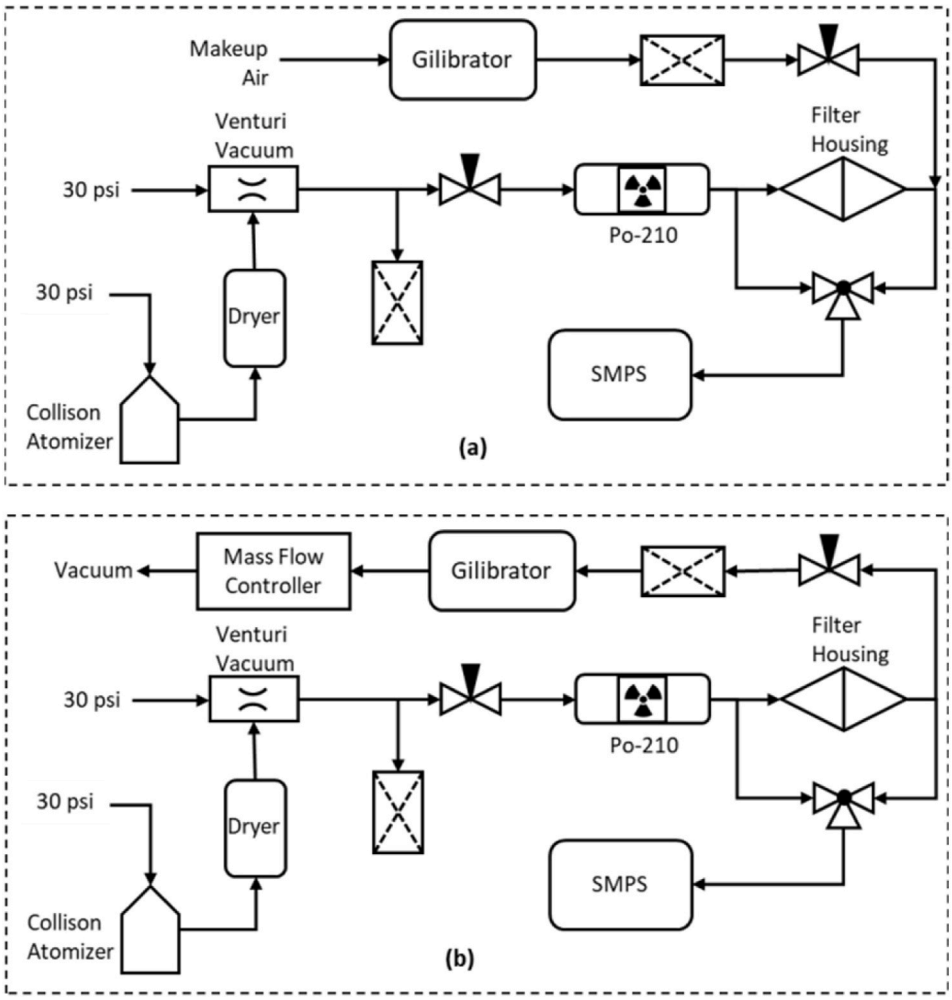

Fig. 1. Filtration efficiency testing configuration for varied face velocities (a) 0.17 cm/s and 0.68 cm/s, (b) 5.3 cm/s and 8.5 cm/s.

can be installed in a building depending on location, local climate, and building characteristics. As many residential houses are built without a central mechanical system worldwide, researchers attempted to replace glass windows with a filter medium. Liu et al. (2015) and Khalid et al. (2017) developed a blow-spinning technique to coat the window screen with nanofibers at a low cost so that fine particles can be filtered passively (Xia et al., 2018). Cheng et al. (2018) applied nanofiber filter windows and Kang et al. (2020) examined four window screen filter materials to evaluate the filtration effect. Before glass was made or imported to East Asia, many Eastern Asian countries such as Korea and Japan used paper windows and doors (see Figure S1). Hanji is a traditional Korean paper made from the inner bark of a mulberry tree. Hanji has translucent permeability to light and porous nature that increases the delivery of light and fresh outdoor air. However, the effects of Hanji paper windows on outdoor pollutant control are not well known. There were some previous studies in literature on the property of the Hanji paper, and most of the papers focused on reliability and aging of the Hanji paper (Choi et al., 2012; Jeong et al., 2014; Kim and Park, 2016). Kim et al. (2020) have shown that the Hanji paper reflects 50% of visible light and transmits 30% of visible light indoors, which provides good visual comfort. During the Covid 19 pandemic in Korea, there were certified mask products made of Hanji paper, reflecting Hanji paper as a good potential filter medium. However, detailed filtration characteristics were not reported in scientific journals. Given this background, the objective of this study is to investigate the filtration characteristics of Hanji paper in laboratory conditions and apply them to full-scale building simulations to evaluate the overall performance of paper filter windows for control of outdoor-originated particles at building scale.

2. Methods

The physical characteristics of Hanji paper and its efficacy to perform as a filtration medium in a passively ventilated home were examined. Physical structure, including fiber diameter and porosity, were measured based on scanning electron microscopy (SEM). The SEM images were processed with ImageJ, a public domain Java image processing program that calculates a distance or area based on selected pixels. Furthermore, pressure drops and size resolved filtration efficiency were measured with the change of the face velocity. Based on the experimentally derived results, outdoor-indoor particle transport was simulated for a full-scale test house. The results reveal how paper filter windows affect ventilation rate and outdoor-indoor particle transport for a residential building.

2.1. Experimental methods

To measure the permeability of Hanji paper samples, a mass flow controller (Alicat MCR-50SLPM) was used to vary the face velocity to the Hanji paper, while a differential pressure gauge (Magnehelic, Dwyer) measured and recorded the pressure difference between the upstream and downstream (see Figure S2).

Using the measurement data of the pressure differences and the flow

Fig. 2. Building layout and the CONTAM model with window openings (Rim et al., 2013a).

rates, the permeability was calculated based on Darcy's law, $\kappa = -Q\mu L/A(P_2 - P_1)$, where κ is the permeability, Q is the flow rate, μ is the dynamic viscosity of air, L is the thickness of the filter, A is the cross-sectional area, P_1 is the pressure upstream of the filter, and P_2 is the pressure downstream of the filter.

To measure particle size distributions upstream and downstream of each paper, a TSI Nanoscan 3910 scanning mobility particle sizer (SMPS) was employed. The Hanji paper's filter efficiency was determined for velocities that were consistent with typical ventilation requirements corresponding to a residential dwelling. The air exchange rates used in this study were 0.1 h^{-1}, 0.4 h^{-1}, and 5.0 h^{-1}, and their corresponding face velocities for a 150 m^3 test house were 0.169 cm/s, 0.677 cm/s, and 8.47 cm/s, respectively. In addition, the standard face velocity for testing filters, 5.3 cm/s, was also examined for a filter area of 11.34 cm^2 (Zhang et al., 2019).

To generate airborne particles for the filtration test, oxygenated hydrocarbon nanoparticles were produced in a Collison-type atomizer using a solution containing dioctyl sebacate ($C_{26}H_{50}O_4$) dissolved in isopropyl alcohol at a concentration of 50 ppm. The particles were brought into charge equilibrium before they encountered the filter media by using radioactive polonium-210 to better represent the conditions that the window material would experience while in use. Each size distribution measurement took a minute and three scans for each condition were taken, alternated between upstream and downstream of the filter. The collection efficiency (η) was then calculated by, $\eta = 1 - C_D/C_U$, where C_U is the upstream concentrations, and C_D is the downstream concentrations.

For the smaller air exchange rates of 0.1 h^{-1} and 0.4 h^{-1}, the SMPS required an intake flow rate that exceeded the low-flow condition. To correct this, filtered make-up air was added to the system and controlled by a needle valve. The filtered airflow rate was monitored by using a Gilian Gilibrator-2 bubble flowmeter. In the case of 5 h^{-1}, a vacuum-powered mass flow controller provided the additional flow (see Fig. 1).

Scanning electronic microscopy (SEM) images of two different Hanji paper material samples were taken. These images were evaluated using ImageJ software. The fiber diameter was determined using the SEM calibrated scale bar in the images. In order to determine the porosity, the software required the user to highlight the surface layer of the image where the surface was interpreted by the brightness. The brightness intensity of the image was mapped onto the threshold control, as shown in Figure S5(b). A range was determined by selecting a low-end and a high-end threshold of the estimated surface area, and Figure S5(c) & (d) show an example of these limits. Porosity was determined by the ratio of bright and dark areas in Figure S5(c) & (d). This analysis was peformed for three images to get an average value.

2.2. Modeling of outdoor-indoor transport for a full-scale building

By inputting the measured data of the filtration efficiency to a multi-zone contaminant transport model in CONTAM (Rim et al., 2013a; Rim et al., 2013b), a full-scale house was simulated for Los Angeles, CA. The multi-zone model calculated airflow through building envelopes and airflow between internal zones and simulates particle transport for each particle size bin. The full-scale building model consisted of four areas: living space, crawl space, belly space, and attic (see Fig. 2). The living space was divided into several zones, and the indoor airflow rates between adjacent zones were calculated. The number concentrations of particles in the living room were used to analyze the effect of the Hanji paper as a representative indoor space while having windows on both north and south walls.

The simulation conditions were designed to examine how the window materials affected air exchange rate and particle concentration (Chan et al., 2005; Feijó-Muñoz et al., 2019; Karava et al., 2007; Rim et al., 2010; Roetzel et al., 2010; Tanrura, 1975; Van Hooff and Blocken,

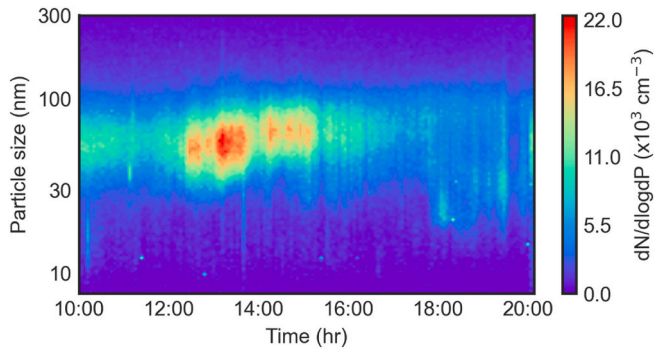

Fig. 3. Particle size distribution measured in Los Angeles.

Table 1
Summary of simulation cases.

Case	Number of open windows (3150 cm^2)	Window material	Glazing ratio (%)
1	0	Glass	50
2	2 (1 north, 1 south)	Glass	50
3	1 (north)	Glass	50
4	1 (south)	Glass	50
5	0	Hanji	50
6	0	Hanji	30

2010; Weidt, 1980). The glazing ratio is the percentage of window area among the total exterior wall area, and two glazing ratios of 30% and 50% were examined. The effective window leakage areas were calculated using an orifice equation based on ISO 5167–1:2003, $q_m = \pi C_d \varepsilon d^2 \sqrt{2\Delta p \rho_1}/(4\sqrt{1-\beta^4})$, where C_d is the coefficient of discharge, β is the diameter ratio of internal orifice diameter d to pipe diameter D, ε is the expansibility factor, ρ_1 is the fluid density, and Δp is the pressure difference. The calculated effective leakage areas were 8 cm^2 for a single glass window and 60 cm^2 for the Hanji paper window.

After determining the leakage area, the penetration factors of conventional window and Hanji window were considered in the simulations. The penetration factor varies with particle size due to their distinct physical and electrical characteristics (Chen et al., 2012; Lai and Nazaroff, 2000; Liu and Nazaroff, 2001; Liu and Nazaroff, 2003; Nazaroff, 2004; Powers, 2009). According to the measured filter efficiency of Hanji, size-resolved penetration factors were inputted in the simulation along with outdoor particle size distribution ranging from 5 to 300 nm measured in Los Angeles as contaminant data inputs (Fig. 3). (Kim and Park, 2010) The outdoor concentration is separated into six bin sizes for simulations using original data. TMY2 weather data were used for the outdoor temperature, humidity, and wind conditions (see Figure S6).

Simulation cases that represent different window opening conditions, window material, and glazing ratios are summarized in Table 1. Case 1 is the baseline condition with glass windows, while Cases 2–4 represent envelope conditions with open windows with different window materials. The rest of the cases (Cases 5–6) reveal the impacts of the glazing ratio on the indoor particle concentration and air exchange rate.

The time-dependent indoor particle size distribution and tracer gas concentrations (SF_6) were obtained as the outputs of the simulations. The air exchange rate of the building was analyzed based on the tracer gas decay of seven consecutive data points over 70 min. Indoor CO_2 concentration was also simulated to examine the ability to remove indoor originated contaminants, especially with Hanji paper windows. With a background CO_2 concentration of 420 ppm, four occupants were simulated with a CO_2 emission rate of 0.005 l/s per person (Kapsalaki, 2022; Persily and de Jonge, 2017). In this paper, the air exchange rate indicates how well the building can remove the indoor-generated contaminants, while indoor particle concentrations reflect how well the windows can filter out particles of outdoor origin.

3. Results

3.1. Hanji filter paper characterization

Based on the SEM and Image J analysis, the fiber diameter was on average ~25 μm with a standard deviation of ±10 μm. The porosity ranged from 45.2 to 73.4%. Fig. 4 shows the filtration efficiencies depending on air exchange rate, for a face velocity of 5.3 cm/s (which corresponds to an air exchange rate of 3.13 h^{-1}). The experimental data were fit to a curve that includes diffusion, interception, impaction, and impaction/interception terms. The curve fits allow the fiber diameter,

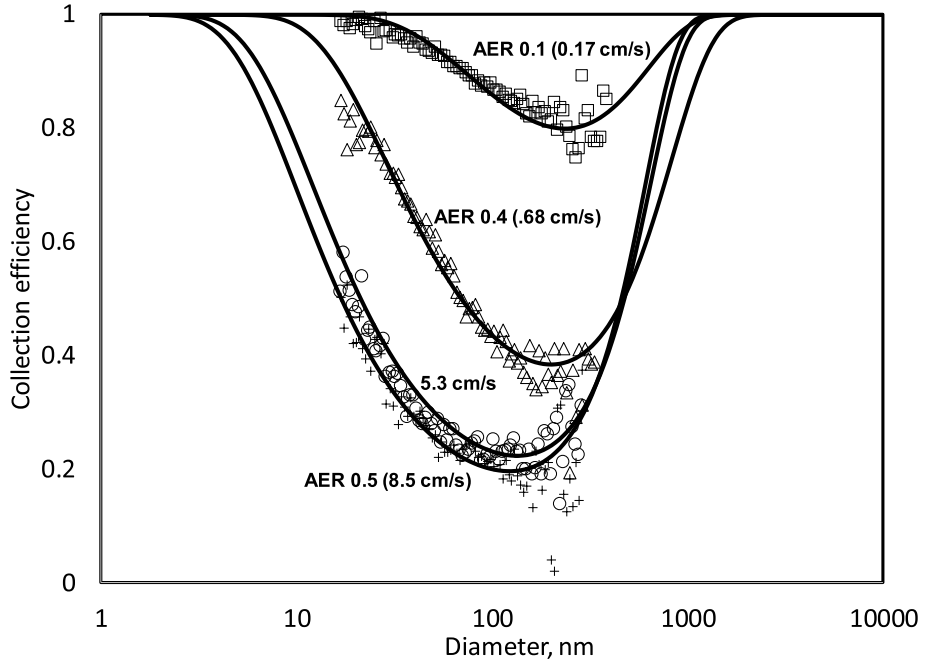

Fig. 4. Filtration efficiencies for Hanji paper windows (regular). Note that AER represents air exchange rate (h^{-1}).

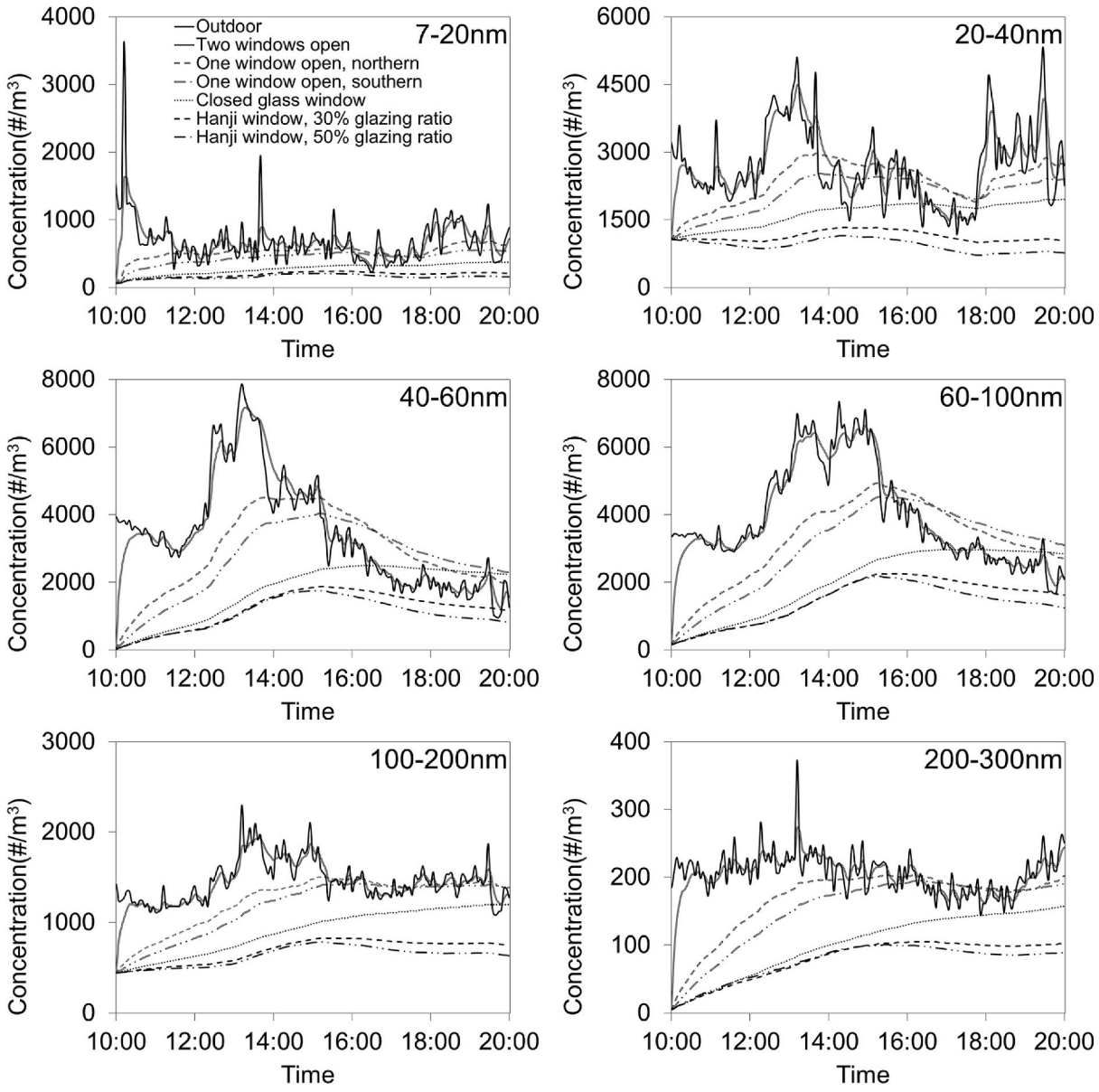

Fig. 5. Size-resolved particle concentration profiles for outdoor all simulation cases.

solidity, peclet constant, and filter thickness to be fitted parameters. The results of the best fit parameters are shown in Table S1. Experimental filtration efficiency results show that for each face velocity setting, there is a most penetrating particle diameter (MPPD) around 100–200 nm. Particles smaller than 100 nm are captured more efficiently as a result of their increased Brownian diffusion. On the other hand, larger particles are captured well due to increases in interception and impaction effects. In summary, the Hanji paper behaves like filter media. The overall filtration efficiency for the regular filter sample was 74% for air exchange rate of 0.1 h^{-1}, 63% for 0.4 h^{-1}, 39% for 3.13 h^{-1} and 38% for 5.0 h^{-1}. Additional information on filtration efficiencies of regular and decorated Hanji papers is provided in Figures S7-8.

3.2. Concentrations of indoor airborne particles of outdoor origin

Based on the outdoor-indoor particle transport simulation results, detailed size-resolved particle concentration profiles are provided in Fig. 5 for the size range of 7–300 nm. The average total number concentration for the baseline case (closed glass windows) is 6750 m^{-3}. When two windows are open, the indoor particle concentration profile closely tracks the outdoor profile, and the average indoor concentration is 12,300 m^{-3}, which is about 83% larger than the baseline case. The case with Hanji paper windows showed the lowest indoor concentrations regardless of particle size.

3.3. Effect of Hanji windows on air change rate

When replacing the glass windows with the Hanji paper windows, the average air exchange rate increases from 0.38 h^{-1} to 0.75 h^{-1} (Fig. 6). The air exchange rate with glass windows was within the range of 0.32 h^{-1} to 0.48 h^{-1}, while the rate with Hanji windows ranged between 0.57 h^{-1} to 1.06 h^{-1}. The air exchange rate with Hanji windows showed a similar time profile to that of an open window, but 75–90% lower than the rates with one open window case.

4. Discussion

The present study evaluated the effectiveness of paper filter windows for controlling the penetration of outdoor particles into buildings. Fig. 7 compares detailed reductions of outdoor particle concentrations due to

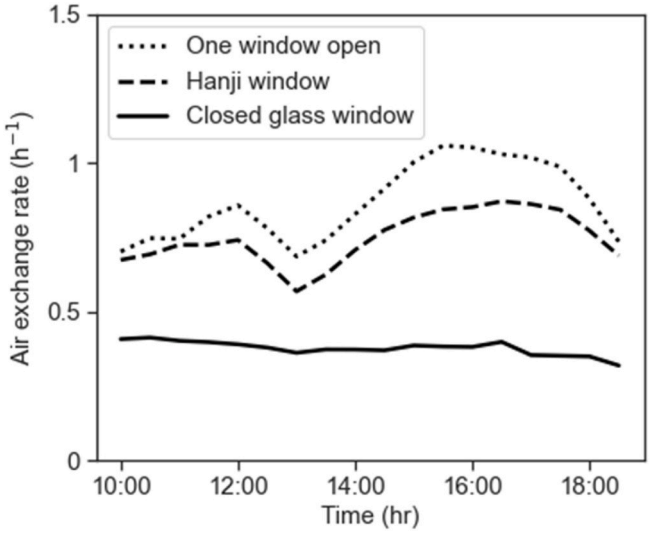

Fig. 6. Time-varying air exchange rates.

conventional glass windows and Hanji paper windows. The reductions of outdoor particles are in the range of 37–59% for the closed glass windows (Case 1), while they are minimal (0.7–2.8%) with two windows open (Case 2). For all particle sizes considered, the particle reduction was the largest with Hanji paper windows with the size-resolved reductions of outdoor particles about 77% for 7–20 nm, 65% for 20–40 nm, 69% for 40–60 nm, 66% for 60–100 nm, 57% for 100–200 nm, and 63% for 200–300 nm. The results also indicate that regardless of the window type, particle concentration reduction is the largest for the smallest size bin (7–20 nm), while it is the lowest for the size bin of 100–200 nm. Overall, the results suggest that Hanji paper windows can function as a filter medium and introduce fewer outdoor particles to the indoor environment, thereby helping reduce indoor concentrations of outdoor-originated particles during severe outdoor air pollution events. David et al. (Ben-David and Waring, 2016) showed that the median value of $PM_{2.5}$ concentration for mechanical ventilation with a minimum efficiency reporting value of 8 (MERV8) filter is about 15% lower than natural ventilation when the minimum ventilation is applied to a building. Therefore, 57–77% particle reductions observed herein due to simply replacing glass windows with Hanji paper windows are noteworthy. Such paper filter window applications will be useful for cities and communities impacted by frequent wildfire events and urban air pollution. Note that the results for the MERV8 filter reported by David et al. (Ben-David and Waring, 2016) were for the same ventilation rate; however, in fact, the Hanji paper windows lead to the increase of the air exchange rate and dilute indoor air contaminants as shown in Fig. 8..

Fig. 8 illustrates the detailed effects of Hanji windows on indoor CO_2 concentration assuming four indoor occupants in the house. With glass windows, the indoor CO_2 concentration reaches 1440 ppm, while the concentration stays below 900 ppm with the Hanji windows.

This trend indicates that the paper filter windows can also help improve the indoor air quality by reducing concentrations of indoor-generated pollutants. It is expected that such dilution effect of the paper filter windows will be pronounced as the number of occupants or indoor source emission rates increase.

The overall results suggest that Hanji paper windows can help reduce the penetration of outdoor-originated $PM_{2.5}$ while reducing other indoor-generated pollutants (i.e., CO_2, VOCs, and virus particles) due to the pollutant dilution associated with ventilation rate increase (Pei et al., 2021). Such findings imply that paper filter windows have

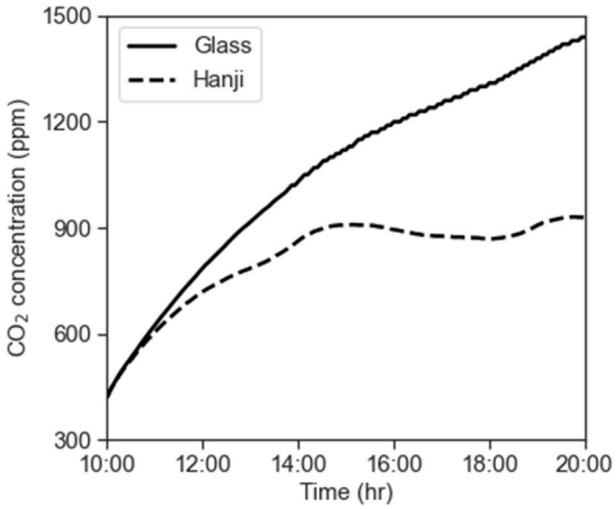

Fig. 8. Size-resolved particle reduction rate for simulation cases.

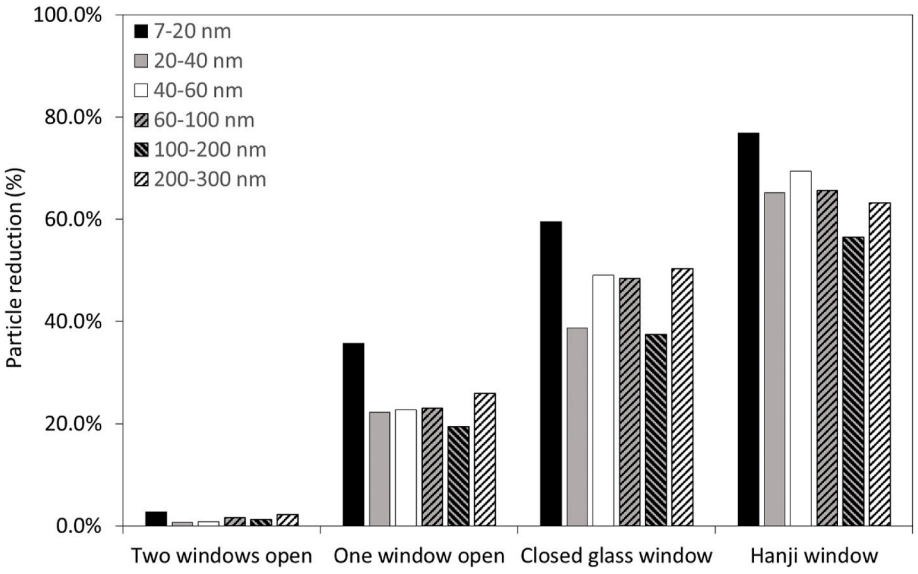

Fig. 7. Size-resolved particle reduction rate for simulation cases.

potential benefits for controlling both indoor-generated and outdoor-originated pollutants with minimal energy inputs, especially in cities and communities impacted by wildfires and urban air pollution. Note that paper filter windows can be applied to single-skin or double-skin facades. While paper windows are preferably operated in temperate climates, future research can explore the combined use of paper and glass windows as a double-skin facade depending on outdoor conditions and seasons. Furthermore, future studies are warranted to explore nanofiber materials and their filtration and thermal characteristics for applications to buildings.

Authorship contribution statement

Suwhan Yee: Data curation; Formal analysis; Investigation; Methodology; Software Validation; Visualization, Writing - review & editing, **Jason Spitzack:** Formal analysis; Investigation; Methodology; Visualization, **Jacob Swanson:** Investigation; Methodology; Software; Supervision, Writing - review & editing, **Heejung Jung:** Conceptualization; Project administration, Writing - review & editing, **Donghyun Rim:** Conceptualization, Supervision, Writing - review & editing.

Declaration of competing interest

The authors declare that they have no known competing financial interests or personal relationships that could have appeared to influence the work reported in this paper.

Data availability

Data will be made available on request.

Acknowledgements

The research presented in this paper was partially supported by the U.S. National Science Foundation (Award No. NSF Grant 1944325). The authors thank Drs. Gwi-Nam Bae and Seung-Bok Lee for providing the first batch of Hanji papers for the laboratory test. The authors would also like to thank Drs. Yifang Zhu and David Quiros for sharing particle size distribution data from their previous studies in Los Angeles, CA.

Appendix A. Supplementary data

Supplementary data to this article can be found online at https://doi.org/10.1016/j.envpol.2023.121996.

References

Ben-David, T., Waring, M.S., 2016. Impact of natural versus mechanical ventilation on simulated indoor air quality and energy consumption in offices in fourteen US cities. Build. Environ. 104, 320–336.
Brook, R.D., Rajagopalan, S., Pope III, C.A., Brook, J.R., Bhatnagar, A., Diez-Roux, A.V., et al., 2010. Particulate matter air pollution and cardiovascular disease: an update to the scientific statement from the American Heart Association. Circulation 121 (21), 2331–2378.
Chan, W.R., Nazaroff, W.W., Price, P.N., Sohn, M.D., Gadgil, A.J., 2005. Analyzing a database of residential air leakage in the United States. Atmos. Environ. 39 (19), 3445–3455.
Chen, C., Zhao, B., Zhou, W., Jiang, X., Tan, Z., 2012. A methodology for predicting particle penetration factor through cracks of windows and doors for actual engineering application. Build. Environ. 47, 339–348.
Chen, H., Samet, J.M., Bromberg, P.A., Tong, H., 2021. Cardiovascular health impacts of wildfire smoke exposure. Part. Fibre Toxicol. 18 (1), 1–22.
Cheng, Z., Cao, J., Kang, L., Luo, Y., Li, T., Liu, W., 2018. Novel transparent nano-pattern window screen for effective air filtration by electrospinning. Mater. Lett. 221, 157–160.
Choi, J.I., Chung, Y.J., Lee, K.S., Lee, J.W., 2012. Effect of radiation on disinfection and mechanical properties of Korean traditional paper, Hanji. Radiat. Phys. Chem. 81 (8), 1051–1054.
Dutton, S.M., Banks, D., Brunswick, S.L., Fisk, W.J., 2013. Health and economic implications of natural ventilation in California offices. Build. Environ. 67, 34–45.
Feijó-Muñoz, J., González-Lezcano, R.A., Poza-Casado, I., Padilla-Marcos, M.Á., Meiss, A., 2019. Airtightness of residential buildings in the Continental area of Spain. Build. Environ. 148, 299–308.
Gall, E.T., Chen, A., Chang, V.W.C., Nazaroff, W.W., 2015. Exposure to particulate matter and ozone of outdoor origin in Singapore. Build. Environ. 93, 3–13.
Jeong, M.J., Kang, K.Y., Bacher, M., Kim, H.J., Jo, B.M., Potthast, A., 2014. Deterioration of ancient cellulose paper, Hanji: evaluation of paper permanence. Cellulose 21 (6), 4621–4632.
Kang, K., Kim, T., Shin, C.W., Kim, K., Kim, J., Lee, Y.G., 2020. Filtration efficiency and ventilation performance of window screen filters. Build. Environ. 178, 106878.
Kapsalaki, M., 2022. ASHRAE Position Document on Indoor Carbon Dioxide.
Karava, P., Stathopoulos, T., Athienitis, A.K., 2007. Wind-induced natural ventilation analysis. Sol. Energy 81 (1), 20–30.
Khalid, B., Bai, X., Wei, H., Huang, Y., Wu, H., Cui, Y., 2017. Direct blow-spinning of nanofibers on a window screen for highly efficient PM2. 5 removal. Nano Lett. 17 (2), 1140–1148.
Kim, T.J., Park, J.S., 2010. Natural ventilation with traditional Korean opening in contemporary house. Build. Environ. 45 (1), 51–57.
Kim, M.O., Park, T.Y., 2016. The manufacture and physical properties of Hanji composite nonwovens utilizing the hydroentanglement process. Fibers Polym. 17 (6), 932–939.
Kim, J.W., Lee, J.H., Kim, K.L., Ryu, J.H., 2020. The impact of total radiation flux on organic materials under LED lighting. J. Conserv. Sci. 36 (4), 236–243.
Klepeis, N.E., Nelson, W.C., Ott, W.R., Robinson, J.P., Tsang, A.M., Switzer, P., et al., 2001. The National Human Activity Pattern Survey (NHAPS): a resource for assessing exposure to environmental pollutants. J. Expo. Sci. Environ. Epidemiol. 11 (3), 231–252.
Lai, A.C., Nazaroff, W.W., 2000. Modeling indoor particle deposition from turbulent flow onto smooth surfaces. J. Aerosol Sci. 31 (4), 463–476.
Licina, D., Tian, Y., Nazaroff, W.W., 2017. Inhalation intake fraction of particulate matter from localized indoor emissions. Build. Environ. 123, 14–22.
Liu, D.L., Nazaroff, W.W., 2001. Modeling pollutant penetration across building envelopes. Atmos. Environ. 35 (26), 4451–4462.
Liu, D.L., Nazaroff, W.W., 2003. Particle penetration through building cracks. Aerosol Sci. Technol. 37 (7), 565–573.
Liu, C., Hsu, P.C., Lee, H.W., Ye, M., Zheng, G., Liu, N., et al., 2015. Transparent air filter for high-efficiency PM2. 5 capture. Nat. Commun. 6 (1), 1–9.
Marshall, J.D., Granvold, P.W., Hoats, A.S., McKone, T.E., Deakin, E., Nazaroff, W.W., 2006. Inhalation intake of ambient air pollution in California's South Coast Air Basin. Atmos. Environ. 40 (23), 4381–4392.
McGuinn, L.A., Ward-Caviness, C., Neas, L.M., Schneider, A., Di, Q., Chudnovsky, A., et al., 2017. Fine particulate matter and cardiovascular disease: comparison of assessment methods for long-term exposure. Environ. Res. 159, 16–23.
Mullen, N.A., Bhangar, S., Hering, S.V., Kreisberg, N.M., Nazaroff, W.W., 2011a. Ultrafine particle concentrations and exposures in six elementary school classrooms in northern California. Indoor Air 21 (1), 77–87.
Mullen, N.A., Liu, C., Zhang, Y., Wang, S., Nazaroff, W.W., 2011b. Ultrafine particle concentrations and exposures in four high-rise Beijing apartments. Atmos. Environ. 45 (40), 7574–7582.
Nazaroff, W.W., 2004. Indoor particle dynamics. Indoor Air 14 (Suppl. 7), 175–183.
Pei, G., Taylor, M., Rim, D., 2021. Human exposure to respiratory aerosols in a ventilated room: Effects of ventilation condition, emission mode, and social distancing. Sustain. Cities Soc. 73, 103090.
Persily, A., de Jonge, L., 2017. Carbon dioxide generation rates for building occupants. Indoor Air 27 (5), 868–879.
Powers, D.A., 2009. Aerosol Penetration of Leak Pathways: an Examination of the Available Data and Models (No. SAND2009-1701). Sandia National Laboratories (SNL), Albuquerque, NM, and Livermore, CA (United States).
Quiros, D.C., Zhang, Q., Choi, W., He, M., Paulson, S.E., Winer, A.M., et al., 2013. Air quality impacts of a scheduled 36-h closure of a major highway. Atmos. Environ. 67, 404–414.
Rim, D., Wallace, L., Persily, A., 2010. Infiltration of outdoor ultrafine particles into a test house. Environ. Sci. Technol. 44 (15), 5908–5913.
Rim, D., Persily, A., Emmerich, S., Dols, W.S., Wallace, L., 2013a. Multi-zone modeling of size-resolved outdoor ultrafine particle entry into a test house. Atmos. Environ. 69, 219–230.
Rim, D., Wallace, L.A., Persily, A.K., 2013b. Indoor ultrafine particles of outdoor origin: importance of window opening area and fan operation condition. Environ. Sci. Technol. 47 (4), 1922–1929.
Rim, D., Gall, E.T., Kim, J.B., Bae, G.N., 2017. Particulate matter in urban nursery schools: a case study of Seoul, Korea during winter months. Build. Environ. 119, 1–10.
Ristovski, Z.D., Miljevic, B., Surawski, N.C., Morawska, L., Fong, K.M., Goh, F., Yang, I. A., 2012. Respiratory health effects of diesel particulate matter. Respirology 17 (2), 201–212.
Roetzel, A., Tsangrassoulis, A., Dietrich, U., Busching, S., 2010. A review of occupant control on natural ventilation. Renew. Sustain. Energy Rev. 14 (3), 1001–1013.
Ruan, T., Rim, D., 2019. Indoor air pollution in office buildings in mega-cities: effects of filtration efficiency and outdoor air ventilation rates. Sustain. Cities Soc. 49, 101609.
Schweizer, C., Edwards, R.D., Bayer-Oglesby, L., Gauderman, W.J., Ilacqua, V., Juhani Jantunen, M., et al., 2007. Indoor time–microenvironment–activity patterns in seven regions of Europe. J. Expo. Sci. Environ. Epidemiol. 17 (2), 170–181.
Stabile, L., Dell'Isola, M., Russi, A., Massimo, A., Buonanno, G., 2017. The effect of natural ventilation strategy on indoor air quality in schools. Sci. Total Environ. 595, 894–902.
Tanrura, C., 1975. Measurement of Air Leakage Characteristics of House Enclosures.

Turanjanin, V., Vučićević, B., Jovanović, M., Mirkov, N., Lazović, I., 2014. Indoor CO2 measurements in Serbian schools and ventilation rate calculation. Energy 77, 290–296.

Van Hooff, T., Blocken, B., 2010. On the effect of wind direction and urban surroundings on natural ventilation of a large semi-enclosed stadium. Comput. Fluids 39 (7), 1146–1155.

Wang, X.R., Gao, H.O., 2011. Exposure to fine particle mass and number concentrations in urban transportation environments of New York City. Transport. Res. Transport Environ. 16 (5), 384–391.

Weidt, J., 1980. Air Leakage of Newly Instaled Residential Windows (No. LBL-11111). Minnesota Energy Agency, St. Paul (USA); Weidt (John) Associates, Inc., Minneapolis, MN (USA). Twin City Testing and Engineering Lab., Inc., St. Paul, MN (USA).

Xia, T., Bian, Y., Zhang, L., Chen, C., 2018. Relationship between pressure drop and face velocity for electrospun nanofiber filters. Energy Build. 158, 987–999.

Xiang, J., Weschler, C.J., Wang, Q., Zhang, L., Mo, J., Ma, R., et al., 2019. Reducing indoor levels of "outdoor PM2. 5" in urban China: impact on mortalities. Environ. Sci. Technol. 53 (6), 3119–3127.

Yamamoto, N., Shendell, D.G., Winer, A.M., Zhang, J., 2010. Residential air exchange rates in three major US metropolitan areas: results from the Relationship Among Indoor, Outdoor, and Personal Air Study 1999–2001. Indoor Air 20 (1), 85–90.

Zhang, S., Rind, N.A., Tang, N., Liu, H., Yin, X., Yu, J., Ding, B., 2019. Electrospun nanofibers for air filtration. In: Electrospinning: Nanofabrication and Applications. William Andrew Publishing, pp. 365–389.